PHYSICAL REVIEW B VOLUME 47, NUMBER 7 15 FEBRUARY 1993-I

Molecular-resolution imaging of insulating macromolecules with the scanning tunneling microscope via a nontunneling, electric-field-induced mechanism

S. L. Tang, A. J. McGhie, and A. Suna
Du Pont Central Research and Development, P.O. Box 80356, Wilmington, Delaware 19880-0356
(Received 22 July 1992; revised manuscript received 16 October 1992)

The scanning tunneling microscope (STM) has been used to obtain molecular-resolution images of a film of hydroxypropylcellulose at least hundreds of angstroms thick in ultrahigh vacuum. Microfibrils with a periodicity of 34 Å were observed directly. The pulsing current used to obtain these images was drastically different from the stable direct current in conventional STM imaging of conducting substrates based on tunneling. An electric-field-induced impurity-mediated conduction in insulating thin-film materials is invoked to explain the occurrence of the pulsing current used for imaging. The experimental resolution in the images was shown to be consistent with the proposed mechanism.

I. INTRODUCTION

The scanning tunneling microscope[1] (STM) offers the unique potential for investigating simultaneously the structural and electronic properties of organic macromolecules. However, the interpretation of the images remains difficult because of a lack of understanding of the imaging mechanism. We describe the STM imaging of a thin film of hydroxypropylcellulose (HPC) in ultrahigh vacuum (UHV). Ordered crystalline microfibrils with a $\sim$34-Å period were observed directly as surface features of a film at least several hundred angstroms in thickness. The observation of a pulsing current accompanying the images showed that the existing proposed mechanisms, whether based on electron tunneling,[2–4] an ion-assisted conduction,[5] or an enhanced conductivity of injected electrons through electronic energy relaxation in a disordered system,[6] could not explain the images. We propose in this paper a nontunneling, field-induced, impurity-mediated electronic-conduction mechanism for imaging surface topographical and electrical and/or electronic structures of a large range of insulating materials with angstrom-scale resolution.

II. EXPERIMENT

Hydroxypropylcellulose is a semisynthetic, semirigid polysaccharide. Like DNA,[7] HPC dissolves in water, and forms lyotropic liquid crystal phases at some critical concentrations.[8] It may be viewed as a model for its natural biological analog and for the technologically important liquid-crystalline polymers such as the aromatic polyamides.[9] In addition, the HPC thin-film morphology may be relevant to the recent interest in studying polymer thin films for chemical separation, bioreactor, etc.[10]

The HPC film was reported to be partially crystalline. The existence of a crystalline microfibril with a diameter of $\sim$34 Å and a length of $\sim$470 Å was proposed based on x-ray line broadening analysis.[11] A sample of HPC (molecular weight $\sim$100 000) for STM studies was prepared by manually dipping a freshly cleaved sample of highly oriented pyrolytic graphite (HOPG) for 60–90 sec in a dilute solution of HPC (0.7 mg/ml) in distilled water. The sample was then warmed on a hot plate at $\sim$70 °C for 1 h before being loaded into the STM in the UHV chamber (operational pressure $\sim 5\times10^{-10}$ torr) through a load-lock system. All the results on HPC were obtained in UHV. Some relevant results mentioned but not described in detail below were obtained either with a home-built STM or a commercial microscope (Nanoscope II) in ambient atmosphere.

III. RESULTS

A. The pulsing current for imaging

The most significant result in this study was that at large film thickness and with modest tip bias voltages ($<\pm4$ V), a *non-direct current* (non-dc) made up of large-amplitude, short-duration current pulses with abrupt onset and termination was observed. These pulses appeared to respond sensitively to the tip positions. Figure 1 presents the time response of the current to the tip position. The current, which is represented by the lower trace, remained at zero until the tip had traversed the final few angstroms to reach the critical position with respect to the sample surface, where the current pulse abruptly surged from zero to its maximum value of over 15 nA. In response to this large current surge, the tip was withdrawn by 75 Å from the original position in 1.2 ms, at which point the current dropped abruptly from $\sim$5 nA to zero. At any specific lateral location of the surface, the tip position with respect to the sample at which the pulse started, the pulse width, and the pulse current amplitude remained fairly constant over tens of seconds, our typical observation time. The current pulse characteristics changed predictably by changing the time constant of the feedback loop electronics by three orders of magnitude, indicating that the pulsing current was not a feedback-loop-related artifact. For instance, decreasing the time constant of the feedback loop, which increased the speed at which the tip changed positions, decreased the current pulse widths and amplitudes, and increased

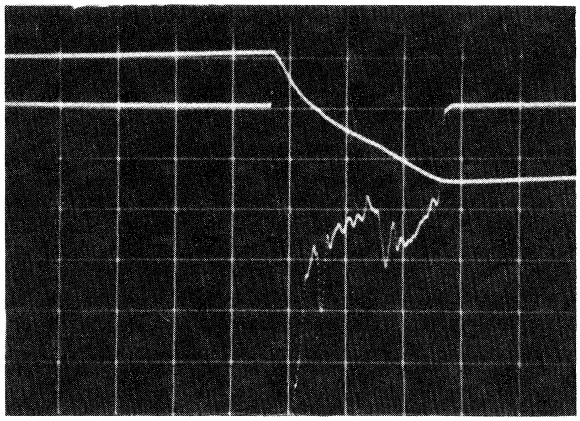

FIG. 1. A storage scope trace of the current (lower trace) vs tip position (upper trace) of the non-dc current obtained on the thicker area of the HPC film. The tip was stationary in the X-Y plane of the sample, and was moving slowing toward the sample, as indicated by the gentle slope in the top trace before the pulse started. The tip bias voltage was -1 V and the time-averaged set current was 0.3 nA. The dc level was zero for the current trace when the tip was only 2–3 Å from the critical position where the pulse started. The grid resolutions are $X=400$ μs per division, Y (tip position) = 30 Å per division, and Y (current)$=2.5$ nA per division. Total tip excursion away from the sample was 75 Å. The current pulse amplitude and width were >15 nA and 1.2 ms, respectively.

their frequencies. These pulses contrast sharply with the stable, constant dc current typically associated with all previous reports of STM imaging of insulating molecules.

The essentially discontinuous dependence of the current with tip-sample gap distance could not be related to any of the tunneling-related STM imaging mechanisms known in the literature,[2–4] or to the model based on enhanced conductivity through electronic energy relaxation and structural disorder.[6]

The pulsing current could be used to obtain images that showed topographylike features with the "constant current" mode of operation, which in this case utilized the constant time-averaged current of the pulses. Height measurements over 2000 Å were observed in seemingly amorphous areas. In the ordered regions of the film, the resolution of the images taken with the pulsing current was determined to be subnanometer. Figure 2(a) shows an image of a 1500×1500 Å^2 area showing regularly spaced rows with a periodicity of ~34 Å. Our observations therefore directly confirmed the existence of microfibrillar structures ordered into a "supermolecular" structure first proposed in the x-ray study described above. Figure 2(b) is a close-up view of several of these rows. The cross-sectional view shows two distinct regions, the essentially atomically flat areas separated by areas of tip oscillations due to the current pulses. The atomically flat areas appeared to have been imaged with a dc current, the origin of which could have been due to smaller pulses in this area, making it possible for the tip to maintain a dc-like current, as discussed above, or to some material-related property which is not understood at present. The tip bias voltage was 0.8 V and the time-averaged current was 0.3 nA.

When the tip bias voltage was decreased to 0.05 V, the tip was observed to move toward the substrate by over 1000 Å. Upon increasing the tip bias voltage back to 0.8 V and therefore retracting the tip, the same area showed a depression several hundred angstroms deep, as shown in Fig. 2(c). The ordered rows were actually surface structures of a thick polymer layer. This observation showed that a critical bias voltage or electric field was necessary for the pulses to occur. Otherwise, the tip would pierce through the insulating polymer layer until a current could be obtained again.

B. Voltage and set current dependences of the pulsing current

In the noncrystalline areas of the film, a particularly interesting observation in the voltage dependence of the pulsing current is that when the tip bias voltages were raised to $\geq\pm4$ V, the pulsing current switched to an extremely stable dc current. Figures 3(a)–3(e) show the

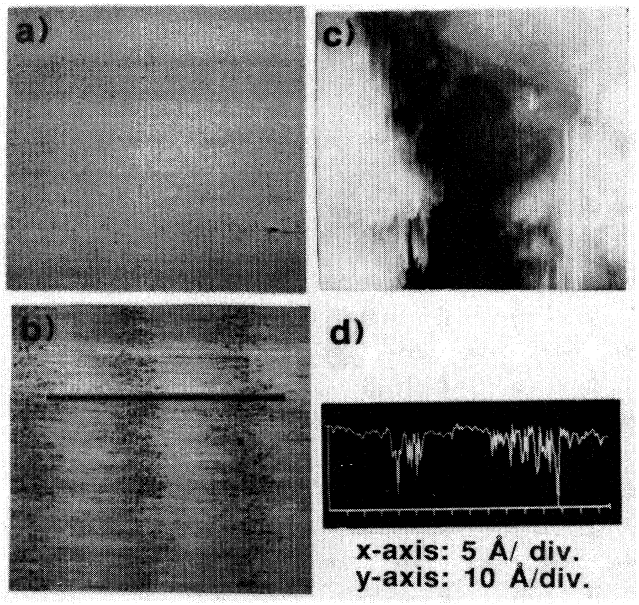

FIG. 2. (a) A 1500×1500 Å^2 image showing rows with a periodicity of ~34 Å. A small defect structure is seen at the lower right-hand corner. The tip bias voltage was -0.8 V and the set current was 0.3 nA. (b) A 100×100 Å^2 view and the cross section of several of these rows. The white areas were essentially atomically flat. The dark areas in (a) were actually due to larger fluctuations of the tip positions in response to larger current pulses in those areas. The largest tip fluctuations were ~10 Å. The black line designates the cross section shown in (d). (c) An elongated depression several hundred angstroms deep was imaged with -0.8 V tip bias voltage in the areas showing microfibrils after the tip bias voltage had been lowered to -0.05 V. The scan area was 6000×6000 Å^2. The depression was elongated in the direction of the axis of the microfibrils. (d) The cross-sectional plot of the microfibrils shown in (b).

evolution of the current pulses with tip bias voltages. The current pulses are represented by their fast Fourier transforms (FFT). The FFT's of the current pulses were obtained at the same spatial location of the film with a spectrum analyzer (Hewlett-Packard 3561A). Each frame represents the average over 100 data samples. The shapes of the FFT wave forms in Figs. 3(b), 3(c), and 3(e)

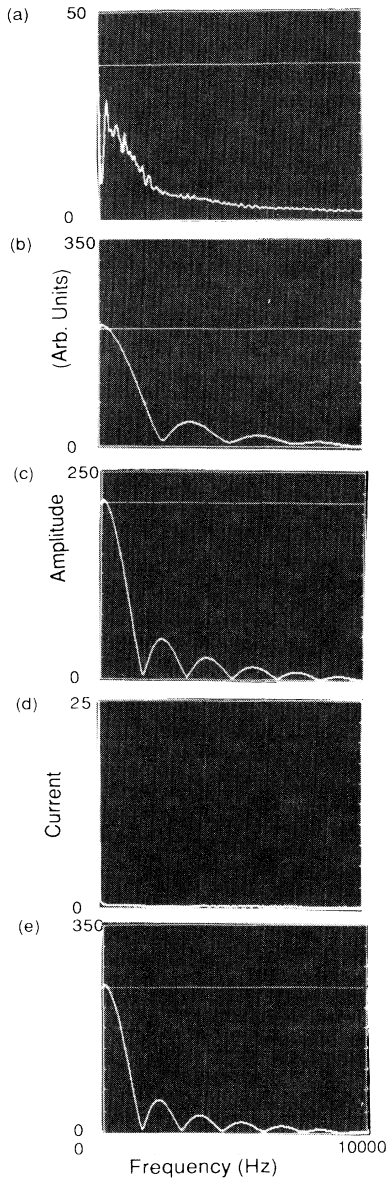

FIG. 3. The FFT's of the current at a single location on the film surface at various tip bias voltages: (a) -0.02 V; (b) -0.2 V; (c) -2 V; (d) -4 V; (e) -2 V. The FFT instead of the time domain signals of the current pulses were shown in order to emphasize the difference between the regular, almost square pulse nature of the current pulses and the nonpulsing current. In the frequency domain, the larger the oscillation period, the smaller the pulse width in the time domain. The vertical scale shown is related to the rms amplitude of the pulses in the time domain.

indicate the presence of well-defined current pulses in the time domain. At -0.02 V tip bias voltage, the current resembles a "noisy" dc-like current, as shown in Fig. 3(a), where no periodic oscillatory wave form can be identified. Well-formed current pulses whose FFT is typified by that in Fig. 3(b) started to occur as the tip bias voltages were increased to more than -0.1 V. Both the duration and the amplitude of the current pulses increased rapidly with further increase in voltages such that the current amplifier (Ithaco 1211) with a dynamic range of 100 nA was saturated. The FFT wave form shown in Fig. 3(c) is characteristic of current amplifier saturation. Essentially the same wave form would persist until the tip bias voltages was increased to close to ~ -4 V, where the current relatively abruptly (within a few hundred millivolts) changed to the quiet dc current, as represented in Fig. 3(d). Lowering the bias voltage from -4 V back to -2 V [Fig. 3(e)] immediately brought back the large current pulses indicating that this transition from the pulsing to the dc current was in fact caused by the change in the level of the tip bias voltage rather than a permanent change in material properties of the film. This observation of the voltage dependence is essentially the same for both voltage polarities, except that for positive tip bias voltages, the transition to dc current was often ~ 0.5 V higher than when negative voltages were used.

We also varied the set time-averaged current of the feedback loop at tip bias voltages where current pulses were small, typically $< \pm 0.1$ V. By increasing the set average current by an order of magnitude, from 0.2 to 2 nA, the current pulses typically increased in amplitude and therefore became more distinct. This observation might have been due to the tip being brought closer to the surface by the feedback loop when the set current was increased at a fixed tip bias voltage. At tip bias voltages where well-formed, large-amplitude current pulses were observed, e.g., ± 2 V, increasing the set average current increased the regularity of the current pulses, and eventually drove the current pulses into resonance at the feedback loop characteristic frequency, several hundred hertz in this case. In this tip bias voltage range, the current pulse amplitude was so much larger than the set average current that increasing the set current by a small amount did not have much effect on the current pulses themselves. We believe that the increased regularity of the current pulses at higher set current was mostly due to the instrumental response of the feedback loop electronics rather than the material itself.

IV. DISCUSSION

A. Electric-field-induced, impurity-mediated conduction

The nontunneling pulsing current that revealed angstrom-scale topographical or electronic features of insulating molecules also revealed important mechanistic aspects of the imaging process. Current pulses similar to those which occurred in the crystalline areas of the HPC film, i.e., relatively small amplitude and high frequency, have been observed in the tunneling current through extremely thin layers, from monolayer to ~ 2 nm, of the ox-

ide of silicon.[12] Those pulses were interpreted as caused by the charging and discharging of surface electron traps in the thin oxide layers. Even though we cannot rule out the possibility of similar charging and discharging of electron traps on our polymer film surface, we must account for the *conduction of a current* through a thick layer of nominally insulating material as well as the current pulses. Pulsing currents in bulk polymer materials are often associated with the diffusional movement in an electric field of the ionic residues commonly found in polymers from their synthesis processes.[13] In order to observe continuous pulses due to continuous motions of the ions, an alternating (ac) voltage is needed to drive the pulsing current. In our experiment where a dc voltage was applied to the tip, repeating pulses at any one location should be accompanied by strong hysteresis,[14] which we did not observe. Also the extremely large current density per pulse, the abrupt onset, and termination of the pulse are not consistent with an ionic diffusion process. Moreover, the previously proposed imaging mechanism due to ionic conductivity in a continuous surface water film[5] can be ruled out because our experiment was conducted in ultrahigh vacuum. It follows that electronic conductivity must have been responsible for the pulse.

Since bulk HPC is an electronic insulator with a band gap of several electron volts, the electronic pulses we observed were extremely unusual. Our dominant experimental observations of the dependence on the tip positions for the onset and the termination of the pulses points to the possibility of an electric-field-induced conduction mechanism. Specifically, the avalanchelike, unstoppable current until the tip or voltage source had been moved far away is characteristic of an electronic breakdown current. In the following we will show that our experimental observations were consistent with an electric-field-induced, electronic-breakdown-like phenomenon.

It has long been recognized that in poorly crystallized materials such as polymers, the incorporated contaminants, and defects play the dominant role in the electronic breakdown process.[15] These chemical and physical defects contribute to states in the band gap close to the conduction-band edge. The energy needed for the electrons from the filled band edge states to be excited into the conduction band is the energy relevant to causing the breakdown event, rather than the band-gap energy of the polymer. This energy can be estimated by adopting a formalism also widely used in treating semiconductors.[16] Inside a dielectric medium, the effective-mass description of an impurity state gives an ionization energy which is inversely proportional to the square of an effective dielectric constant of the medium. Our present observations, where the pulsing current could be observed at a tip bias voltage as low as a few tens of millivolts, imply correspondingly low ionization energies. Since these are smaller than typical vibrational energies, the effective dielectric constant applicable here is the static dielectric constant.[17,18]

Cellulose materials in general have relatively high static dielectric constants[19] in the range 4–8. For HPC, which has many hydroxyl groups, our preliminary measurements of the static dielectric constants at room temperature were in the range $\sim 6.5 - \sim 14$, depending on the moisture content. Thus, contaminant atoms[20] with typical free space ionization energies of several electron volts would have these energies reduced by a factor of >40, consistent with our observations. Under equilibrium conditions, these ionized electrons in the conduction band will *not* result in significant conductivity because the ionized electrons fall back into localized trap states such as chain ends and lose energy to the lattice. However, if a large electric field is applied such that the applied field exceeds the critical field for breakdown, equilibrium can no longer be maintained, and the ionized electrons in the conduction band will gain energy directly from the field faster than they can fall into localized trap states.[21] An electronic runaway, observed as an avalanche current, results.

We have verified that this picture of the field-induced, impurity-mediated conduction is consistent with our observations on polymer materials with a broad range of dielectric constants. For instance, in the imaging of thin layers (~ 900 Å) of fibers of an aromatic polyamide, the critical voltages needed for the pulsing current to occur for imaging the crystalline structure of the fibers were much larger, in the range $\pm 1 - \pm 1.5$ V, consistent with the lower dielectric constant of this material.[22]

As we will discuss in greater detail below, given the right geometry for the tip and the dielectric polymer layer, the nominal bulk breakdown strength of cellulose materials of ~ 50 kV/mm (Ref. 19) could be exceeded by the field created by a tip bias voltage of just 0.05 V to cause an electronic runaway. The trigger for the current flow could easily be provided by the contact between the tip and the polymer surface, or perhaps by tunneling between the tip and the contaminant states in the band gap of the polymer. Once the breakdown has been generated at the surface, the process may then follow physical defects or domain boundaries which likely penetrate the small thickness of the polymer layer to the graphite substrate. This is analogous to bulk electric breakdown in which macroscopic physical defects have to be developed through the thickness of the dielectric before breakdown can occur.[23] The observation of the regions with current pulses defining the microfibrils is also consistent with the observation of breakdown in bulk polymers such as polyethylene where the electronic breakdown has been observed to occur at the boundaries of microcrystalline domains known as spherulites.[24]

As in bulk dielectric breakdown, the process described here as manifested by the pulsing current appeared to be a function of many variables such as tip bias voltage, thickness of the layers, morphology, etc., which may also have interdependences. We have presented detailed results on the voltage dependence of the current pulses in the noncrystalline areas of the layer, i.e., increasing tip bias voltage from about ± 0.05 to ± 3 V increased the current pulse amplitude from several nanoamps to over 100 nA, and the pulse duration ranged from hundreds of microseconds to over 1 ms. However, in the crystalline area of the layer, the pulses appeared to have an opposite voltage dependence. Figure 4 illustrates this point. Figures 4(a) and 4(b) show the same 7400×7400 Å^2 area

taken at −3 V and −0.06 V, respectively. The pulses decreased with voltage such that at −0.06 V, the pulses became so small that the tip oscillations due to the pulses essentially disappeared. In Figs. 4(c) and 4(d), the area was scanned at +0.2 V and 0.03 V, respectively. The tip oscillations that defined the microfibrils were much more prominent at the lower tip bias voltage.

Such complicated dependences of the pulses on the tip bias voltages and the film morphology, and the transition from a pulsing to a quiet dc current at $\sim\pm 4$ V (this transition was also observed in the imaging of the aromatic polyamide fibers at similar tip bias voltages[22]) make the quantitative characterization of the current difficult, and more measurements and extensive modeling will be necessary. However, these observations point to the possibility of utilizing the STM to investigate important and hitherto difficult to handle properties such as the local electrical transport properties of the crystalline versus the amorphous regions of semicrystalline polymers.

It is interesting to examine whether the large amplitude of the current pulses can cause damage to the film. In experiments on the dielectric breakdown of bulk materials where high voltages are applied, material damage is often observed.[25] In this experiment, we never observed material damage due to the pulsing current. One possibility is that the damage could have been beneath the surface of the layer. This is not likely because the pulse height and width remained fairly constant over many pulses. The other possibility for the lack of observable damage could be that the current pulses, because they were regulated by the tip position in a timely fashion through the feedback loop electronics, were too short to cause thermally induced damage. We verified that this is indeed the case by analyzing the energy balance at the location of the pulse with a pseudo two-dimensional thermal diffusion model to mimic the flow of thermal energy through the thin polymer film.[26] For a pulse such as the one shown in Fig. 1, we obtained a temperature difference of ~ 30 K, too low to reach the decomposition temperature of HPC at 200–270 K.[27]

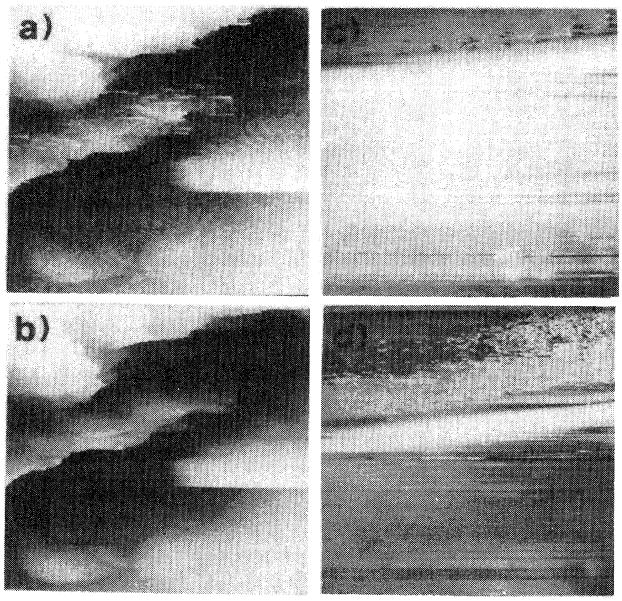

FIG. 4. (a) A 7400×7400 Å^2 scan of a thick HPC film taken at a tip bias voltage of −3 V and 0.3 nA set current. The fine channel-like structures were due to the tip position swinging in response to the large current pulses. The greyscale bar indicates relative height in angstroms. (b) The same area scan as (a). All scan parameters were the same as (a) except that tip bias voltage was lowered to −0.06 V. The channel-like features were not present because of the smaller pulses at this bias voltage. (c) A 300×300 Å^2 scan of an area containing microfibrillar structure at the top of the image. The tip bias voltage was +0.2 V and the set current was 0.3 nA. (d) The same area scan as in (c). The area with microfibrils had drifted toward the center of the scan. The tip bias voltage was lowered to +0.03 V and the set current was 0.3 nA. The tip oscillations due to the pulsing current were much more prominent at this tip bias voltage.

B. Lateral resolution of the proposed imaging mechanism

The question remains whether an electric-field-induced breakdown imaging mechanism could achieve angstrom-scale resolution. We estimate the resolution by calculating the lateral variation of the electric-field strength near the tip directly underneath the surface of a uniform

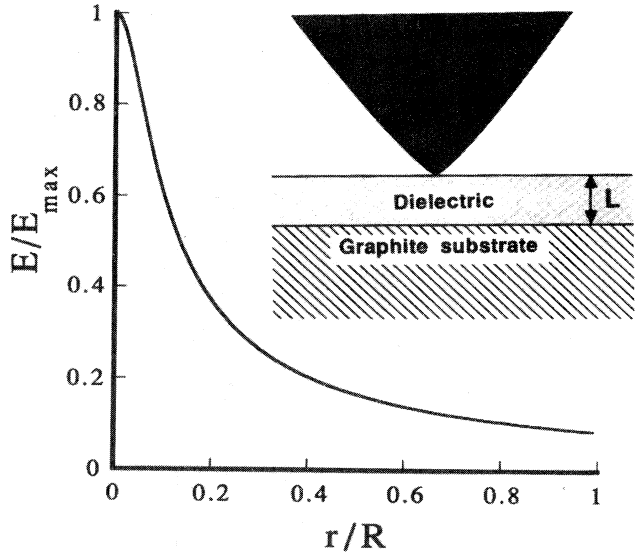

FIG. 5. Calculated electric-field strength normalized to the maximum field E_{max} as a function of distance from the tip apex normalized to the radius of curvature of the tip apex. The dielectric constant of the medium was chosen to be 8. The inset shows pictorially the model used to obtain the plot. The tip shape was chosen (see the Appendix) to coincide with an equipotential of a simple solution of the Maxwell equations near an interface with a uniform dielectric medium. The chosen equipotential surface just touches the dielectric and its radius of curvature at the point of contact is equal to the tip radius R. Another equipotential at a distance L from the tip simulates the substrate at ground potential and is nearly planar for $L \gg R$. The tip surface is shown to a lateral distance of $100R$ away from the tip apex, where it is $\sim 100R$ above the dielectric surface.

dielectric layer when the tip is just touching the surface of the dielectric layer. We investigated a variety of model tip shapes and found that the lateral field distribution, and therefore the lateral resolution, depends primarily on the radius of curvature of the tip and the dielectric constant of the imaged material. The maximum field near the tip varies but slightly also with the specific model for the shape of the tip at distances large compared to the tip radius. The inset in Fig. 5 is the schematic drawing of the representative tip shape (see the Appendix) chosen to evaluate the lateral field distribution shown in Fig. 5. The magnitude of the field just inside the dielectric layer, normalized to the maximum field $E_{\max}$, is plotted as a function of the distance r from the tip apex, normalized to the tip radius. The dielectric constant is assumed to be 8 for this plot. Note that the field distribution falls off sharply at distances smaller than a tip radius. In general, the distance from the tip where $E_{\max}$ is halved is $\sim R/\varepsilon$. The maximum field $E_{\max}$ inside the dielectric layer can be expressed as $\alpha V/R$, where V is the applied voltage on the tip, R is the radius of the tip, and α is a constant that depends on L/R, L being the thickness of the dielectric. α may be as large as ε, the dielectric constant. In other words, the presence of the dielectric enhances the magnitude and decreases the lateral extent of the field in the vicinity of the tip. If we take the value of R/ε to be the upper limit for determining the resolution, then our analysis shows that the subnanometer resolution that we experimentally observed in the microfibril regions would be possible with a very sharp tip in a high dielectric medium such as HPC. In our experiment, R was determined to be indeed very small, 50–100 Å, by measuring the size of the depressions on the substrate made by gently impinging the tip on the substrate. Taking V to be 0.05 V, and ε to be 8, the nominal bulk critical breakdown field of 50 kV/mm could also be reached. The field distribution in Fig. 5 further implies that the resolution should degrade with voltage that is increased beyond the voltage needed to produce the breakdown field. The images in Fig. 4 actually illustrate this point. In both the noncrystalline [Figs. 4(a) and 4(b)] and the crystalline [Figs. 4(c) and 4(d)] regions, the structural features were better resolved with the lower tip bias voltages.

As we mentioned earlier, the model described here appears to be applicable to the macromolecules of drastically different dielectric properties. To further test and perhaps quantify the model, we have initiated experiments in which the polymer materials imaged have been doped with known amounts of chemical dopants. Since the mechanism described above only relies on the abundance of contaminant states close to the band edge and the existence of continuous physical defects between the tip/insulator and insulator/substrate interfaces, we have also attempted to image thin layers of nominally insulating inorganic materials with similar electronic properties by nature or through chemical doping. Our preliminary results on a thin film (nominally 200 Å thick) of Ge-doped Al_2O_3 seem to support this extension of the model because the pulsing current was observed when imaging this material.[28] The occurrence of the pulsing current in a large range of materials with drastically different mechanical properties also suggests that the mechanical pressure from the tip should not play an important role in this imaging mechanism of relatively thick insulating films.

V. SUMMARY

In summary, we have presented molecular-resolution images of a relatively thick film of HPC with the STM. Microfibrils arranged into a supermolecular structure with a periodicity of 34 Å were observed directly for the first time. The pulsing current characteristics point to a nontunneling, chemical defect-mediated dielectric breakdown process of the material. This mechanism does not damage the material as a result of the control of the tip positions. The field-induced conduction model formulated based on our experimental observations predicted that the resolution of the mechanism should be dependent on the dielectric constant of the macromolecular layer, the tip shape and the tip bias voltage, and subnanometer resolution should be possible with the extremely sharp tips used in our experiments. Our results may provide a possible physical basis for the STM images of large insulating organic molecules reported in the literature, since foreign chemical species are often naturally incorporated, and in fact can be difficult to avoid in most of these materials. Furthermore, they suggest the possibilities of chemically doping insulating materials for imaging with the STM, and probing electronic and dielectric properties of the polymers with angstrom-scale resolution.

ACKNOWLEDGMENTS

We thank P. Avakian for the dielectric constant measurements, G. Blackman for XPS measurements, K. S. Lee, C. Jackson, and I. Shah for some of the sample preparations, H. Hsiung and B. Sauer for many valuable suggestions, S. Masur, R. V. Kasowski, J. O'Brien, W. Bindloss, J. Miller, R. Liepins, and Professor A. Epstein for helpful discussions, and L. Heineman for assistance with the software.

APPENDIX: MODEL OF THE FIELD IN THE VICINITY OF AN STM TIP IN CONTACT WITH A DIELECTRIC SUBSTRATE

Given any function $f(x,y,z)$ which is a solution of Laplace's equation in free space, an expression for the potential ϕ when a uniform dielectric medium (with dielectric constant ε) fills the half-space $z<0$ is

$$\phi(x,y,z)=\begin{cases}\frac{1}{2}(1+\varepsilon)f(x,y,z_0-z)+\frac{1}{2}(1-\varepsilon)f(x,y,z_0+z) & \text{for } z>0\\ f(x,y,z_0-z) & \text{for } z<0\ .\end{cases}$$

This solution satisfies the conditions of continuity of ϕ and of $D_z = -\varepsilon\, d\phi/dz$ at $z=0$. We choose a function f such that the equipotential $\phi(x,y,z)=\phi(0,0,0)$, for $z>0$, is a reasonable approximation for a tip shape, then adjust z_0 to give the right radius of curvature R. The function ϕ must not have singularities between the tip equipotential and the ground equipotential, the solution of $\phi(x,y,z)=\phi(0,0,-L)$, where L is the distance between the tip and the conducting substrate.

The specific solution illustrated in Fig. 5 corresponds to $f(x,y,z)=\text{const}\ln(r+z)$, where $r=(x^2+y^2+z^2)^{1/2}$, and $z_0=\frac{1}{2}R/\varepsilon$. The maximum field strength inside the dielectric is given by $E_{\max}=(V/R)\varepsilon[2/\ln(2\varepsilon L/R)]$, where V is the difference in potential between the tip and ground.

[1]G. Binnig, H. Rohrer, Ch. Gerber, and E. Weibel, Phys. Rev. Lett. **50**, 120 (1983).

[2]S. M. Lindsay *et al.*, J. Phys. Chem. **94**, 4655 (1990).

[3]J. K. Spong *et al.*, Nature (London) **338**, 137 (1989).

[4]W. Mitzutani, M. Shigeno, M. Ono, and K. Kajimura, Appl. Phys. Lett. **56**, 1974 (1990).

[5]J.-Y. Yuan, Z. Shao, and C. Gao, Phys. Rev. Lett. **67**, 863 (1991).

[6]R. Garcia and N. Garcia, Chem. Phys. Lett. **173**, 44 (1990).

[7]C. Robinson, Tetrahedron **13**, 219 (1961); E. Lizuka, Polym. J. **9**, 173 (1977).

[8]R. S. Werbowyj and D. G. Gray, Macromolecules **13**, 69 (1980).

[9]M. G. Northolt, Eur. Polym. J. **10**, 799 (1974).

[10]L. Chao and C. R. Martin, Nature (London) **352**, 50 (1991); M. R. Anderson *et al.*, Science **252**, 1412 (1991).

[11]R. J. Samuels, J. Polym. Sci. Part A-2, **7**, 1197 (1969).

[12]M. E. Welland and R. H. Koch, Appl. Phys. Lett. **48**, 724 (1986); R. H. Koch and R. J. Hamers, Surf. Sci. **181**, 333 (1987)

[13]A. R. Blythe, *Electrical Properties of Polymers* (Cambridge University Press, Cambridge, England, 1979), pp. 90–92.

[14]S. M. Sze, *Physics of Semiconductor Devices* (Wiley, New York, 1981), pp. 402–404.

[15]H. Frohlich, Proc. R. Soc. London, Ser. A **188**, 521 (1947).

[16]J. C. Anderson, *Dielectrics* (Reinhold, New York, 1964), pp. 101–102.

[17]C. Kittel, *Introduction to Solid State Physics* (Wiley, New York, 1986), p. 206

[18]J. C. Philips, *Bonds and Bands in Semiconductors* (Academic, New York, 1973) p. 229

[19]*Polymer Handbook*, edited by J. Brandup and E. H. Immergut (Wiley, New York, 1989), p. V/114.

[20]We examined our HPC films with x-ray photoemission spectroscopy (XPS). Substantial amounts (a few percent) of Si-related contaminants were observed. This Si contamination was probably due to the contamination from the packaging materials for the HPC pellets. Because of the low sensitivity of XPS, the natural contaminants of HPC from the synthesis process might not have been detected. The analysis on the distilled water used as solvent showed trace amounts (1–3 ppm) of Cu and Si.

[21]A. R. Blythe, in *Electrical Properties of Polymers* (Ref. 13), pp. 141–146.

[22]Since in this case the ionization energies are higher than typical vibrational energies of the material, the optical dielectric constant in the range 2–3 is more appropriate (see Refs. 14 and 15) than the static dielectric constant of ~3.5 for the screening of the ionization energies of the impurity states. The results for this material will be published elsewhere.

[23]C. C. Ku and R. Liepins, *Electrical Properties of Polymers, Chemical Principles* (Hanser, Munich, 1987), pp. 106–115.

[24]K. Kitagawa, G. Sawa, and M. Ieda, Jpn. J. Appl. Phys. **19**, 389 (1980).

[25]M. Danziger and A. Bernhardt, Phys. Status Solidi B **164**, 569 (1991).

[26]The current going through the layer was described as a Gaussian source. The detailed model using energy balance will be published elsewhere.

[27]*Polymer Handbook* (Ref. 19), p. V/94.

[28]S. L. Tang, A. J. McGhie, and S. I. Shah (unpublished).

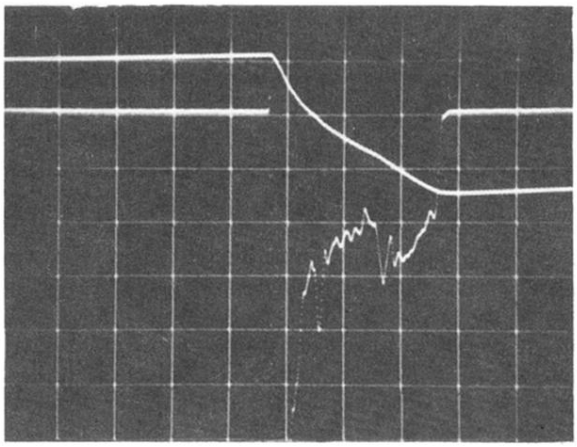

FIG. 1. A storage scope trace of the current (lower trace) vs tip position (upper trace) of the non-dc current obtained on the thicker area of the HPC film. The tip was stationary in the X-Y plane of the sample, and was moving slowing toward the sample, as indicated by the gentle slope in the top trace before the pulse started. The tip bias voltage was -1 V and the time-averaged set current was 0.3 nA. The dc level was zero for the current trace when the tip was only 2–3 Å from the critical position where the pulse started. The grid resolutions are $X = 400$ μs per division, Y (tip position) = 30 Å per division, and Y (current) = 2.5 nA per division. Total tip excursion away from the sample was 75 Å. The current pulse amplitude and width were > 15 nA and 1.2 ms, respectively.

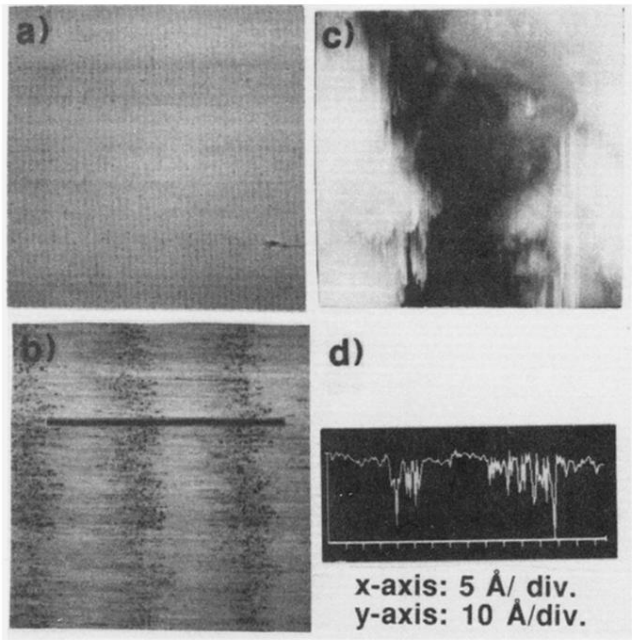

FIG. 2. (a) A 1500×1500 Å^2 image showing rows with a periodicity of ~ 34 Å. A small defect structure is seen at the lower right-hand corner. The tip bias voltage was -0.8 V and the set current was 0.3 nA. (b) A 100×100 Å^2 view and the cross section of several of these rows. The white areas were essentially atomically flat. The dark areas in (a) were actually due to larger fluctuations of the tip positions in response to larger current pulses in those areas. The largest tip fluctuations were ~ 10 Å. The black line designates the cross section shown in (d). (c) An elongated depression several hundred angstroms deep was imaged with -0.8 V tip bias voltage in the areas showing microfibrils after the tip bias voltage had been lowered to -0.05 V. The scan area was 6000×6000 Å^2. The depression was elongated in the direction of the axis of the microfibrils. (d) The cross-sectional plot of the microfibrils shown in (b).

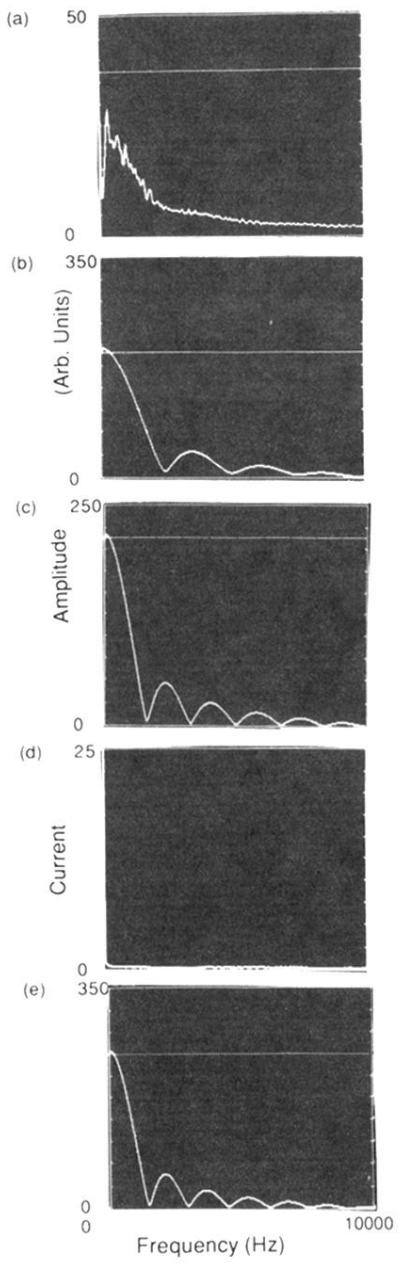

FIG. 3. The FFT's of the current at a single location on the film surface at various tip bias voltages: (a) -0.02 V; (b) -0.2 V; (c) -2 V; (d) -4 V; (e) -2 V. The FFT instead of the time domain signals of the current pulses were shown in order to emphasize the difference between the regular, almost square pulse nature of the current pulses and the nonpulsing current. In the frequency domain, the larger the oscillation period, the smaller the pulse width in the time domain. The vertical scale shown is related to the rms amplitude of the pulses in the time domain.

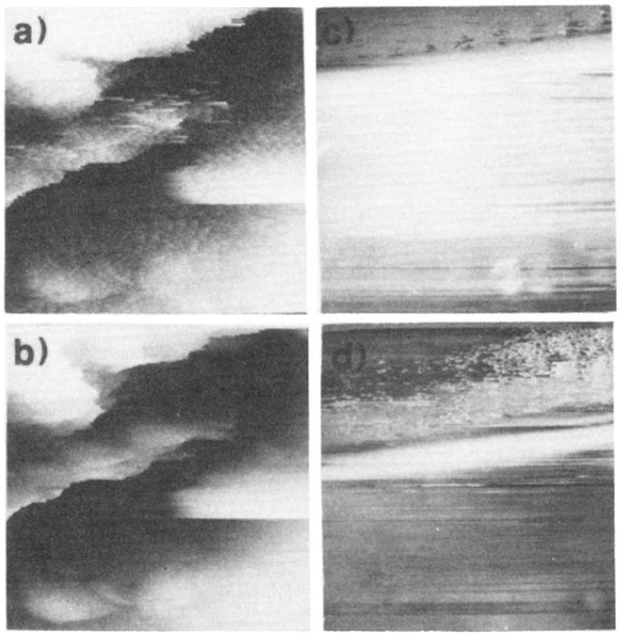

FIG. 4. (a) A 7400×7400 Å^2 scan of a thick HPC film taken at a tip bias voltage of −3 V and 0.3 nA set current. The fine channel-like structures were due to the tip position swinging in response to the large current pulses. The greyscale bar indicates relative height in angstroms. (b) The same area scan as (a). All scan parameters were the same as (a) except that tip bias voltage was lowered to −0.06 V. The channel-like features were not present because of the smaller pulses at this bias voltage. (c) A 300×300 Å^2 scan of an area containing microfibrillar structure at the top of the image. The tip bias voltage was +0.2 V and the set current was 0.3 nA. (d) The same area scan as in (c). The area with microfibrils had drifted toward the center of the scan. The tip bias voltage was lowered to +0.03 V and the set current was 0.3 nA. The tip oscillations due to the pulsing current were much more prominent at this tip bias voltage.

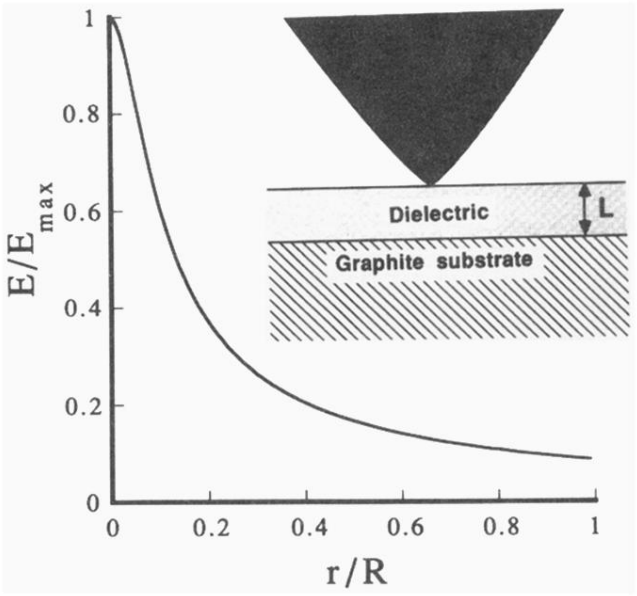

FIG. 5. Calculated electric-field strength normalized to the maximum field E_{max} as a function of distance from the tip apex normalized to the radius of curvature of the tip apex. The dielectric constant of the medium was chosen to be 8. The inset shows pictorially the model used to obtain the plot. The tip shape was chosen (see the Appendix) to coincide with an equipotential of a simple solution of the Maxwell equations near an interface with a uniform dielectric medium. The chosen equipotential surface just touches the dielectric and its radius of curvature at the point of contact is equal to the tip radius R. Another equipotential at a distance L from the tip simulates the substrate at ground potential and is nearly planar for $L \gg R$. The tip surface is shown to a lateral distance of $100R$ away from the tip apex, where it is $\sim 100R$ above the dielectric surface.